Acta Cryst E CRYSTALLOGRAPHIC COMMUNICATIONS

ISSN 2056-9890

Crystal structure and Hirshfeld surface analysis of an erbium(III) coordination polymer based on a 2,3,5,6-tetrabromobenzene-1,4-dicarboxylate ligand

Suwadee Jiajaroen[a]* and Kittipong Chainok[b]

[a]Division of Science and Mathematic, Faculty of Science and Technology, Rajamangala University of Technology Tawan-ok, Bangpra, Sriracha, Chonburi, 20110, Thailand, and [b]Thammasat University Research Unit in Multifunctional Crystalline Materials, and Applications (TU-MCMA), Faculty of Science and Technology, Thammasat University, Khlong Luang, Pathum Thani, 12121, Thailand. *Correspondence e-mail: suwadee_ji@rmutto.ac.th

Received 15 October 2026
Accepted 15 October 2026

Edited by L. Van Meervelt, Katholieke Universiteit Leuven, Belgium

Keywords: crystal structure; coordination polymer; erbium(III); carboxylate.

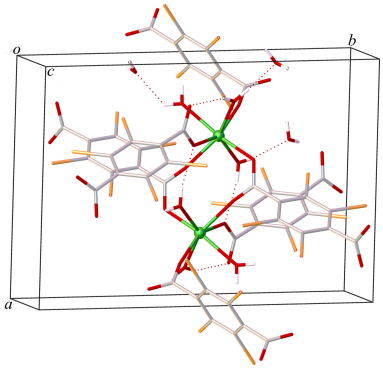
CCDC reference: 2595517

Supporting information: this article has supporting information at journals.iucr.org/e

The title polymeric compound, poly[[triaqua(μ_3-2,3,5,6-tetrabromobenzene-1,4-dicarboxylato)hemi(μ_2-2,3,5,6-tetrabromobenzene-1,4-dicarboxylato)erbium(III)] trihydrate], $\{[Er(C_8Br_4O_4)_{1.5}(H_2O)_3]\cdot 3H_2O\}_n$ or $\{[Er(Br_4bdc)_{1.5}(H_2O)_3]\cdot 3H_2O\}_n$ (**1**), was hydrothermally synthesized and structurally characterized. The asymmetric unit contains one Er^{III} cation, one and a half Br_4bdc^{2-} dianions, three coordinated H_2O molecules, and three uncoordinated solvent H_2O molecules. The central Er^{III} cation is seven-coordinated within a distorted capped trigonal-prismatic geometry. The coordination sphere is defined by four carboxylate oxygen atoms from four Br_4bdc^{2-} ligands and three aqua oxygen atoms. The Br_4bdc^{2-} ligand occupies a general position, and acts as a μ_3-bridge linking three symmetry-related Er^{III} cations. It coordinates *via* μ_3-κO:$\kappa O'$:$\kappa O''$ mode, using its carboxylate oxygen atoms to extend into a two-dimensional polymeric sheet parallel to the *bc* plane. Meanwhile, the remaining Br_4bdc^{2-} ligand is situated on a crystallographic inversion centre and adopts a μ_2-κO:$\kappa O'$ coordination mode linking the sheets into a three-dimensional network. The cohesion of the three-dimensional supramolecular framework is enhanced by classical O–H···O hydrogen bonds. The crystal packing is further consolidated by intermolecular Br···Br and Br···O halogen bonding interactions. The analysis of the Hirshfeld surface reveals that the primary contributions arise from Br···Br (23.5%) and O···H/H···O (20.8%) contacts. Additional contributions include Br···H/H···Br (13.2%), H···C/C···H (12.5%), Br···C/C···Br (8.4%), Br···O/O···Br (7.0%), and O···O (5.3%) interactions.>

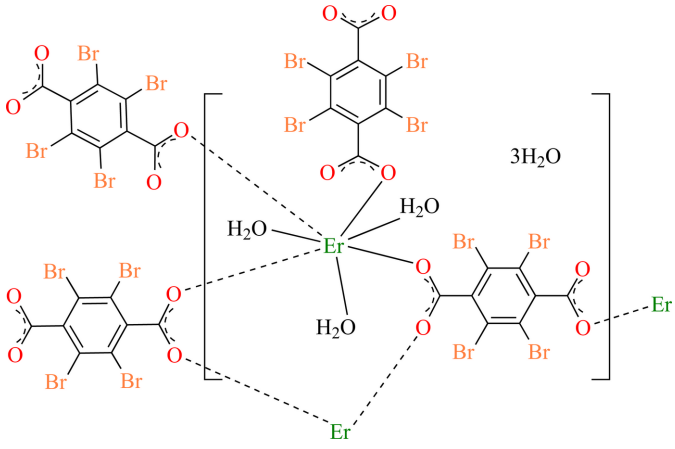
1. Chemical context

Lanthanide coordination polymers (LnCPs) have been widely studied and their potential applications, including electronic, optical, and magnetic properties arising from the unique 4*f* electronic configurations of Ln^{III} ions (Bünzli, 2010; Capelo *et al.*, 2025; Shiels *et al.*, 2026). Unlike transition-metal ions, Ln^{III} ions exhibit high and variable coordination numbers together with a wide range of coordination geometries. They possess robust *Ln*—O bonds and a hard Lewis acid character, resulting in a strong affinity for hard donor atoms, particularly oxygen-containing ligands (Cui *et al.*, 2012; Saraci *et al.*, 2020; Costanzo *et al.*, 2026). These characteristics make Ln^{III} ions attractive building units and provide flexibility in the assembly of structural diversity (Bünzli, 2014; Boone *et al.*, 2024). Besides, the selection of ligands plays a crucial role in constructing diverse topologies and properties. Aromatic polycarboxylic acids are widely employed as organic linkers in the design and construction of CPs. In particular, terephthalic



OPEN ACCESS
Published under a CC BY 4.0 licence

acid (H_2bdc) and its functionalized derivatives display versatile coordination modes spanning monodentate, chelating, bridging, and chelating–bridging fashions, yielding structurally diverse networks upon self-assembly (Li *et al.*, 2014; Jiajaroen *et al.*, 2022; Nisa *et al.*, 2024). Among these derivatives, 2,3,5,6-tetrabromobenzene-1,4-dicarboxylic acid (H_2Br_4bdc) is structurally significant; the four bulky, electronegative bromine substituents drastically alter the steric and electronic environment of the central aromatic core, significantly influencing both the primary coordination spheres and the secondary supramolecular interactions. The presence of bromine substituents may influence the opportunities for intermolecular halogen-related interactions, particularly Br···Br and other halogen-containing contacts. These may play a crucial role in crystal packing and structural stabilization. Herein, we report the synthesis and crystal structure of a new erbium(III) CP, namely, poly[[triaqua(μ_3-2,3,5,6-tetrabromobenzene-4-dicarboxylato)hemi(μ_2-2,3,5,6-tetrabromobenzene-1,4-dicarboxylato)erbium(III)] trihydrate] (**1**). The assembly of the polymeric framework and the supramolecular interactions of **1** are thoroughly elucidated and examined. Furthermore, Hirshfeld surface analysis provides a quantitative evaluation of intermolecular contacts and crystal packing interactions of **1**.



2. Structural commentary

The asymmetric unit of **1** contains one Er^{III} atom, one and a half Br_4bdc^{2-} ligands, three coordinated water molecules, and three uncoordinated water molecules. The Er^{III} ion adopts an [ErO_7] coordination environment with four oxygen atoms from four different Br_4bdc^{2-} ligands and three oxygen atoms from coordinated water molecules (Fig. 1), displaying a distorted capped trigonal-prismatic geometry (CTPR-7; value 4.082) (*SHAPE 2.1*; Llunell *et al.*, 2013). The Er—O bond lengths fall in the range of 2.238 (2) to 2.347 (3) Å, mean 2.304 (2) Å. The O—Er—O bond angles range from 73.11 (8) to 155.44 (11)°. The fully deprotonated Br_4bdc^{2-} ligand exhibits a μ_3-κO:$\kappa O'$:$\kappa O''$ bridging mode, linking three symmetry-related Er^{III} ions to propagate a two-dimensional sheet parallel to the *bc* plane (Fig. 2). Within this layer, the shortest

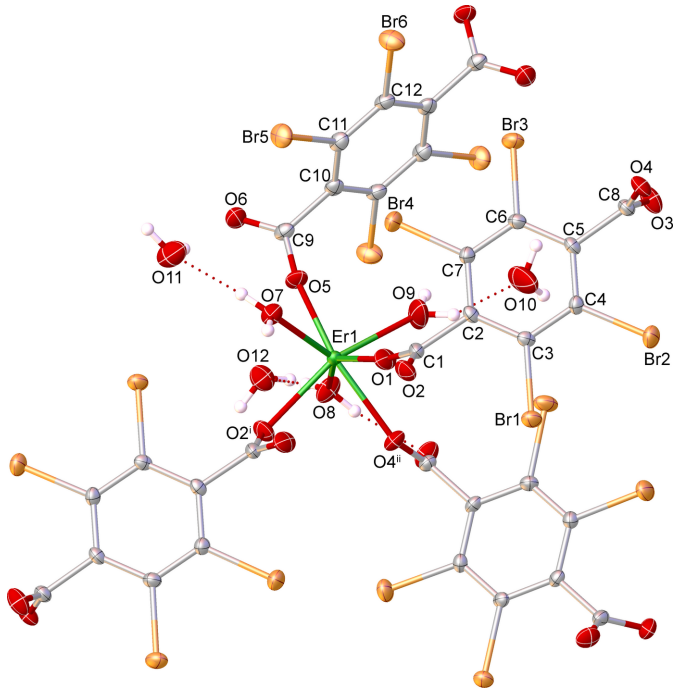


Figure 1
Molecular structure of **1**, showing the asymmetric unit with the atom-labeling scheme and the coordination environment of the Er^{III} ion. Displacement ellipsoids are drawn at the 40% probability level. Symmetry codes: (i) $1-x, 1-y, 2-z$ and $x, \frac{1}{2}-y, \frac{1}{2}+z$.

Er···Er separation is 4.6625 (19) Å. The sheets are further interconnected into a three-dimensional framework along the *c*-axis direction by the remaining Br_4bdc^{2-} ligand, which resides on a crystallographic inversion centre and acts as a μ_2-κO:$\kappa O'$ bridge (Fig. 3).

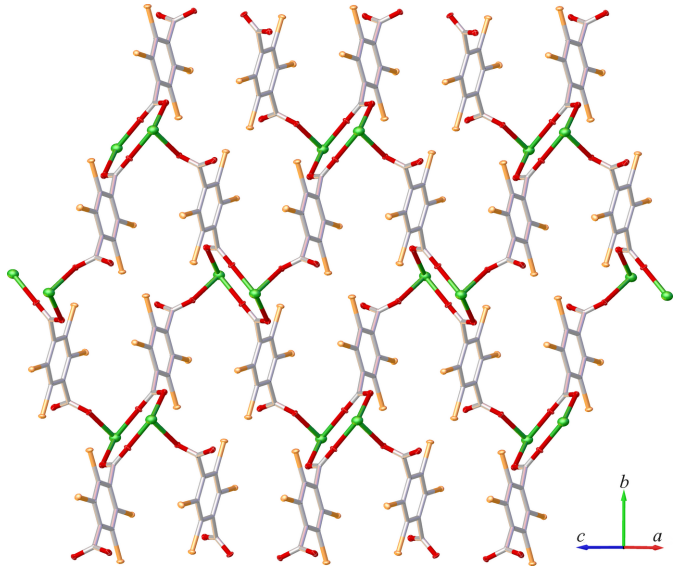


Figure 2
View of the two-dimensional sheet structure of **1** in the *bc* plane.

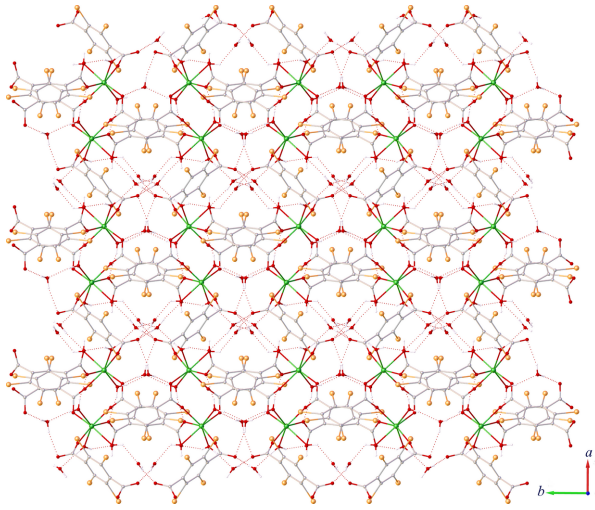


Figure 3
View of the three-dimensional framework of **1** along the *c* axis.

3. Supramolecular features

In the crystal structure, the coordinated water molecules (O7*W*, O8*W* and O9*W*) act as hydrogen-bond donors, forming robust intermolecular O—H···O hydrogen-bonding interactions with the water molecules of crystallization (O10*W*, O11*W* and O12*W*) serving as the hydrogen-bond acceptors (Table 1). Moreover, the carboxylate oxygen atoms of the Br_4bdc^{2-} ligands serve as hydrogen-bond acceptors for the solvent water molecules, contributing to the cohesion of the supramolecular network (Fig. 4). The crystal packing is further consolidated by intermolecular Br···Br and Br···O halogen bonding interactions (Table 2) occurring between adjacent Br_4bdc^{2-} ligands. No significant π–π stacking interactions are observed between neighboring benzene rings, as the centroid-to-centroid separations fall well outside the typical 3.3–3.8 Å range characteristic of such supramolecular contacts (Janiak, 2000).

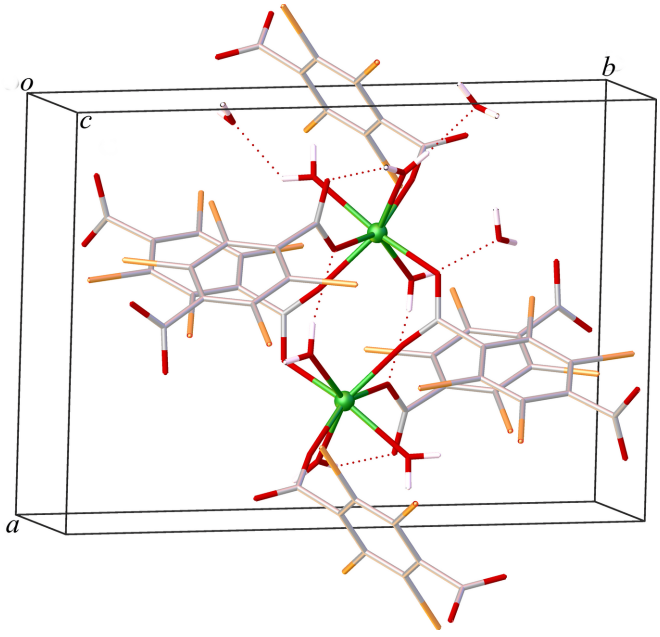


Figure 4
View of the O—H···O hydrogen bonds involving the carboxylate groups of the Br_4bdc^{2-} ligands and water molecules of **1**. Hydrogen-bonding interactions are shown as dashed lines.

Table 1
Hydrogen-bond geometry (Å, °).

D—H···*A*	*D*—H	H···*A*	*D*···*A*	*D*—H···*A*
O7—H7*A*···O11	0.86 (3)	2.06 (3)	2.892 (4)	165 (5)
O7—H7*B*···O4^{i}	0.84 (3)	2.10 (3)	2.931 (4)	168 (4)
O8—H8*A*···O12	0.84 (3)	1.86 (3)	2.705 (4)	174 (3)
O8—H8*B*···O3^{ii}	0.82 (4)	1.96 (3)	2.703 (3)	152 (5)
O9—H9*A*···O10	0.84 (2)	2.05 (4)	2.643 (5)	128 (4)
O10—H10*A*···O12^{iii}	0.85 (3)	2.00 (5)	2.808 (4)	160 (5)
O10—H10*B*···O6^{iii}	0.84 (5)	2.12 (6)	2.948 (5)	171 (6)
O11—H11*A*···O6	0.84 (3)	2.18 (4)	2.989 (4)	161 (5)
O11—H11*B*···O2^{i}	0.84 (5)	2.31 (5)	3.139 (4)	174 (6)
O12—H12*A*···O3^{iv}	0.84 (4)	2.06 (4)	2.879 (4)	164 (4)
O12—H12*B*···O6^{v}	0.84 (4)	1.99 (4)	2.832 (3)	177 (4)

Symmetry codes: (i) $-x+1, y+\frac{1}{2}, -z+\frac{3}{2}$; (ii) $x, -y+\frac{1}{2}, z+\frac{1}{2}$; (iii) $-x, y-\frac{1}{2}, -z+\frac{3}{2}$; (iv) $-x, y+\frac{1}{2}, -z+\frac{3}{2}$; (v) $x, -y+\frac{3}{2}, z+\frac{1}{2}$.

Table 2
Br···*X* halogen-bond geometry (Å, °).

C—Br···*X*	Br···*X*	C—Br···*X*	Type
C4—Br2···Br2^{i}	3.7489 (14)	129.40 (7)	I
C6—Br3···Br6	3.8861 (11)	134.30 (8)	II
C7—Br4···Br2^{ii}	3.7048 (13)	120.25 (8)	I
C7—Br4···Br5	3.5390 (15)	161.06 (8)	II
C11—Br5···Br1^{ii}	3.5739 (15)	174.31 (9)	II
C3—Br1···O11^{iii}	3.054 (3)	160.04 (10)	
C12—Br6···O3^{iv}	3.265 (3)	175.75 (9)	

Symmetry codes: (i) $1-x, -y, 2-z$; (ii) $1-x, \frac{1}{2}+y, \frac{3}{2}-z$; (iii) $1-x, 1-y, 2-z$; (iv) $x, \frac{1}{2}-y, -\frac{1}{2}+z$.

4. Hirshfeld surface analysis

A Hirshfeld surface analysis was carried out using *CrystalExplorer* (Spackman *et al.*, 2021) to examine the intermolecular interactions in **1**. The 3D Hirshfeld surface mapped over d_{norm} highlights close intermolecular contacts as red spots, whereas white and blue regions correspond to contacts close to and longer than the sum of the van der Waals radii, respectively (Fig. 5). The analysis of the two-dimensional fingerprint plots (Fig. 6) reveals that the largest contribution arises from Br···Br contacts (23.5%), indicating that close halogen···halogen contacts constitute a significant feature of the crystal packing. The O···H/H···O contacts (20.8%) correspond to the extensive network of O–H···O hydrogen bonds involving carboxylate oxygen atoms, coordinated aqua ligands, and solvent water molecules. Secondary contributions to the Hirshfeld surface area include Br···H/H···Br (13.2%) and H···C/C···H (12.5%) contacts, which further consolidate the supramolecular architecture. Minor packing contributions are attributed to Br···C/C···Br (8.4%), Br···O/O···Br (7.0%), O···O (5.3%) and O···C/C···O (4.2%) contacts. Notably, C···C contacts account for only 0.7% of the Hirshfeld surface area, corroborating the absence of significant π–π

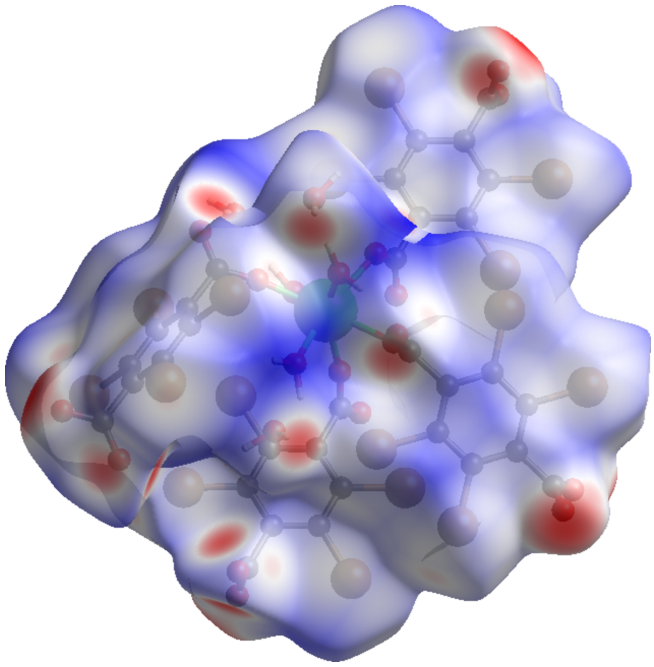


Figure 5
View of the Hirshfeld surface for **1** plotted over d_{norm}.

stacking interactions within the crystal structure. Therefore, it can be concluded that halogen and hydrogen bonds are the major intermolecular contacts that contribute to the consolidation of the crystal packing of **1**.

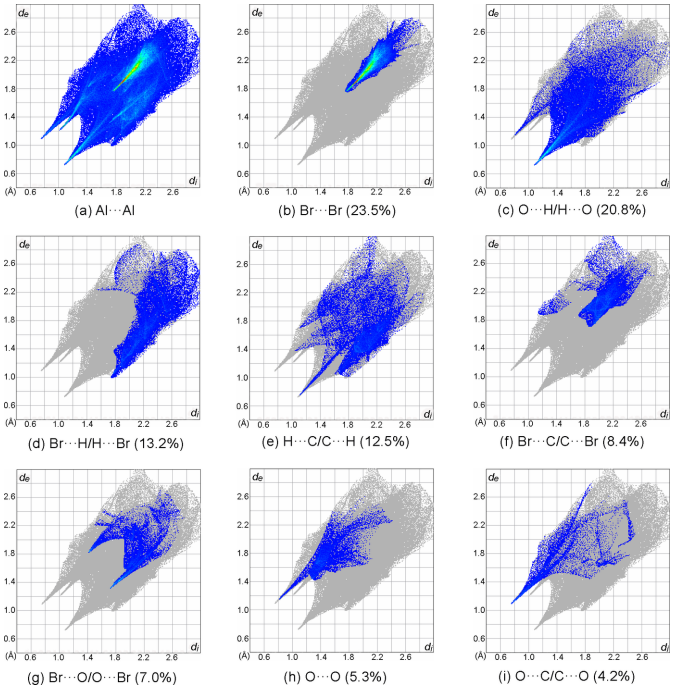


Figure 6
The two-dimensional fingerprint plots for **1**, showing (*a*) all interactions, and those delineated into (*b*) Br···Br, (*c*) O···H/H···O, (*d*) Br···H/H···Br, (*e*) H···C/C···H, (*f*) Br···C/C···Br, (*g*) Br···O/O···Br, (*h*) O···O, and (i) O···C/C···O interactions. The d_e and d_i values represent the closest external and internal distances (Å), respectively, from a given point on the Hirshfeld surface.

Table 3
Experimental details.

Crystal data	
Chemical formula	$[Er(C_8Br_4O_4)_{1.5}(H_2O)_3]\cdot 3H_2O$
M_r	994.94
Crystal system, space group	Monoclinic, $P2_1/c$
Temperature (K)	296
a, b, c (Å)	12.711 (5), 15.839 (6), 12.906 (5)
β (°)	113.171 (15)
V (Å^3)	2388.9 (17)
Z	4
Radiation type	Mo $K\alpha$
μ (mm^{-1})	13.60
Crystal size (mm)	0.14 × 0.12 × 0.1
Data collection	
Diffractometer	Bruker D8 QUEST CMOS PHOTON II
Absorption correction	Multi-scan (*SADABS*; Krause *et al.*, 2015)
T_{min}, T_{max}	0.571, 0.746
No. of measured, independent and observed [$I > 2\sigma(I)$] reflections	98614, 5854, 5331
R_{int}	0.055
(sin $\theta/\lambda)_{max}$ (Å^{-1})	0.664
Refinement	
$R[F^2 > 2\sigma(F^2)]$, $wR(F^2)$, S	0.019, 0.046, 1.17
No. of reflections	5854
No. of parameters	324
No. of restraints	17
H-atom treatment	Only H-atom coordinates refined
$\Delta\rho_{max}$, $\Delta\rho_{min}$ (e Å^{-3})	0.50, −1.21

Computer programs: *APEX6* and *SAINT* (Bruker, 2023), *SHELXT2014/5* (Sheldrick, 2015*a*), *SHELXL2018/3* (Sheldrick, 2015*b*) and *OLEX2* (Dolomanov *et al.*, 2009).

5. Database survey

A search of the Cambridge Structural Database (CSD version 6.01, September 2026 update; Groom *et al.*, 2016) for the structures of lanthanide complexes incorporating Br_4bdc^{2-} ligands yielded 47 hits. Among these, thirteen structures, including SITROE and SITROE01 (Wei *et al.*, 2014; Smith *et al.*, 2019), BIQMAS, BIQMEW, BIQMIA, BIQMUM, BIQNAT, BIQNEX, BIQNIB, and BIQNOH (Smith *et al.*, 2019), FECFOM, FECFUS, and FECGAZ (Jiajaroen *et al.*, 2022), display concurrent μ_2-κO:$\kappa O'$ and μ_3-κO:$\kappa O'$:$\kappa O''$ coordination modes of the Br_4bdc^{2-} ligands to bind the Ln^{III} centres. Furthermore, the complexes BIQNUN, BIQPAV, BIQPEZ, BIQPID, and BIQPOJ (Smith *et al.*, 2019) exclusively exhibit the μ_3-κO:$\kappa O'$:$\kappa O''$ bridging mode, whereas NICZOQ (Lv *et al.*, 2013*a*), WIPXUQ, and WIPYAX (Lv *et al.*, 2013*b*) display only the μ_2-κO:$\kappa O'$ coordination mode to bind the Ln^{III} cations.

6. Synthesis and crystallization

All starting materials and reagents were of analytical grade and were used as received without further purification. A mixture of $Er(NO_3)_3\cdot 5H_2O$ (44.3 mg, 0.1 mmol) and H_2Br_4bdc (48.2 mg, 0.1 mmol) was dissolved in a solvent mixture of methanol (1 mL) and distilled water (3 mL) in a 15 mL Teflon-lined reactor. The mixture solution was stirred at room temperature for 10 min, sealed in stainless steel autoclave, and

heated under autogenous pressure in a temperature-controlled oven at 373 K for 48 h. After the autoclave had cooled slowly to ambient temperature, the reaction mixture was filtered, and the filtrate was transferred to a glass vial. Slow evaporation of the mother liquor at room temperature over approximately one week yielded pink block-shaped crystals. Yield: 12.4 mg, 28% based on the $Er(NO_3)_3{\cdot}5H_2O$.

7. Refinement

Crystal data, data collection and structure refinement details are summarized in Table 3. The hydrogen atoms were located from difference electron-density maps. H atoms bonded to O atoms were refined with distance restraints O—H = 0.84 ± 0.02 Å and with U_{iso}(H) = 1.5U_{eq}(O) for H9*A*/*B* and H10*A*/*B* and independently refined for eight other atoms.

Acknowledgements

This project was partially supported by the Thammasat University Research Unit in Multifunctional Crystalline Materials and Applications (TU-MCMA).

References

Boone, M., Artizzu, F., Goura, J., Mara, D., Van Deun, R. & D'hooghe, M. (2024). *Coord. Chem. Rev.* **501**, 215525.
Bruker (2023). *APEX6* and *SAINT*. Bruker AXS Inc., Madison, Wisconsin, USA.
Bünzli, J.-C. G. (2010). *Chem. Rev.* **110**, 2729–2755.
Bünzli, J.-C. G. (2014). *J. Coord. Chem.* **67**, 3706–3733.
Capelo, R. G., Garcia, F. D. R., Strutynski, C., Désévédavy, F., Gadret, G., da Silva, C. M., Arroyos, G., Frem, R. C. G., Orellana, G., Smektala, F. & Manzani, D. (2025). *ACS Appl. Mater. Interfaces* **17**, 70667–70679.
Costanzo, M., Bianco, S., Fik-Jaskółka, M. & Roviello, G. N. (2026). *Int. J. Mol. Sci.* **27**, 1566.
Cui, Y., Yue, Y., Qian, G. & Chen, B. (2012). *Chem. Rev.* **112**, 1126–1162.
Dolomanov, O. V., Bourhis, L. J., Gildea, R. J., Howard, J. A. K. & Puschmann, H. (2009). *J. Appl. Cryst.* **42**, 339–341.
Groom, C. R., Bruno, I. J., Lightfoot, M. P. & Ward, S. C. (2016). *Acta Cryst.* B**72**, 171–179.
Janiak, C. (2000). *J. Chem. Soc. Dalton Trans.* pp. 3885–3896.
Jiajaroen, S., Dungkaew, W., Kielar, F., Sukwattanasinitt, M., Sahasithiwat, S., Zenno, H., Hayami, S., Azam, M., Al-Resayes, S. I. & Chainok, K. (2022). *Dalton Trans.* **51**, 7420–7435.
Krause, L., Herbst-Irmer, R., Sheldrick, G. M. & Stalke, D. (2015). *J. Appl. Cryst.* **48**, 3–10.
Li, M., Li, D., O'Keeffe, M. & Yaghi, O. M. (2014). *Chem. Rev.* **114**, 1343–1370.
Llunell, M., Casanova, D., Cirera, J., AlemPny, A. & Alvarez, S. (2013). *SHAPE*. University of Barcelona, Barcelona, Spain.
Lv, X.-Y., Ye, Q., Liu, Y., Liu, J.-F., Gao, L.-L. & Hu, T.-P. (2013*a*). *Jiegou Huaxue* **32**, 439–445.
Lv, X.-Y., Ye, Q., Qiao, J.-Z., Wu, J.-Y., Liu, J.-F., Xiao, L.-Q. & Hu, T.-P. (2013*b*). *Jiegou Huaxue* **32**, 1185–1193.
Nisa, Z. U., Ahmad, M. & Sheikh, H. N. (2024). *New J. Chem.* **48**, 3100–3109.
Saraci, F., Quezada-Novoa, V., Donnarumma, P. R. & Howarth, A. J. (2020). *Chem. Soc. Rev.* **49**, 7949–7977.
Sheldrick, G. M. (2015*a*). *Acta Cryst.* A**71**, 3–8.
Sheldrick, G. M. (2015*b*). *Acta Cryst.* C**71**, 3–8.
Shiels, D., Gunarathna, N., Brennessel, W. W. & Matson, E. M. (2026). *Inorg. Chem.* **65**, 12557–12573.
Smith, J. A., Singh-Wilmot, M. A., Carter, K. P., Cahill, C. L. & Ridenour, J. A. (2019). *Cryst. Growth Des.* **19**, 305–319.
Spackman, P. R., Turner, M. J., McKinnon, J. J., Wolff, S. K., Grimwood, D. J., Jayatilaka, D. & Spackman, M. A. (2021). *J. Appl. Cryst.* **54**, 1006–1011.
Wei, L., Ye, Y. & Zhang, R. (2014). *J. Mol. Struct.* **1058**, 51–55.

supporting information

Acta Cryst. (2026). E**82**, 1323-1327 [https://doi.org/10.1107/S2056989026010698]

Crystal structure and Hirshfeld surface analysis of an erbium(III) coordination polymer based on a 2,3,5,6-tetrabromobenzene-1,4-dicarboxylate ligand

Suwadee Jiajaroen and Kittipong Chainok

Computing details

Poly[[triaqua(μ_3-2,3,5,6-tetrabromobenzene-1,4-dicarboxylato)hemi(μ_2-2,3,5,6-tetrabromobenzene-1,4-dicarboxylato)erbium(III)] trihydrate]

Crystal data

$[Er(C_8Br_4O_4)_{1.5}(H_2O)_3]\cdot 3H_2O$
M_r = 994.94
Monoclinic, $P2_1/c$
a = 12.711 (5) Å
b = 15.839 (6) Å
c = 12.906 (5) Å
β = 113.171 (15)°
V = 2388.9 (17) Å^3
Z = 4
$F(000)$ = 1832
D_x = 2.766 Mg m^{-3}
Mo $K\alpha$ radiation, λ = 0.71073 Å
Cell parameters from 8607 reflections
θ = 3.1–28.1°
μ = 13.60 mm^{-1}
T = 296 K
Block, pink
0.14 × 0.12 × 0.1 mm

Data collection

Bruker D8 QUEST CMOS PHOTON II diffractometer
Radiation source: sealed x-ray tube
Graphite monochromator
Detector resolution: 7.39 pixels mm^{-1}
φ and ω scans
Absorption correction: multi-scan (SADABS; Krause *et al.*, 2015)
T_{min} = 0.571, T_{max} = 0.746
98614 measured reflections
5854 independent reflections
5331 reflections with $I > 2\sigma(I)$
R_{int} = 0.055
θ_{max} = 28.2°, θ_{min} = 3.1°
h = −16→16
k = −21→21
l = −17→17

Refinement

Refinement on F^2
Least-squares matrix: full
$R[F^2 > 2\sigma(F^2)]$ = 0.019
$wR(F^2)$ = 0.046
S = 1.17
5854 reflections
324 parameters
17 restraints
Hydrogen site location: difference Fourier map
Only H-atom coordinates refined
$w = 1/[\sigma^2(F_o^2) + (0.0183P)^2 + 2.0786P]$ where $P = (F_o^2 + 2F_c^2)/3$
$(\Delta/\sigma)_{max}$ = 0.002
$\Delta\rho_{max}$ = 0.50 e Å^{-3}
$\Delta\rho_{min}$ = −1.21 e Å^{-3}

Special details

Geometry. All esds (except the esd in the dihedral angle between two l.s. planes) are estimated using the full covariance matrix. The cell esds are taken into account individually in the estimation of esds in distances, angles and torsion angles; correlations between esds in cell parameters are only used when they are defined by crystal symmetry. An approximate (isotropic) treatment of cell esds is used for estimating esds involving l.s. planes.

Fractional atomic coordinates and isotropic or equivalent isotropic displacement parameters (Å²)

	x	*y*	*z*	U_{iso}*/U_{eq}
Er1	0.30558 (2)	0.53186 (2)	0.91422 (2)	0.01547 (4)
Br1	0.53394 (2)	0.20275 (2)	1.02462 (2)	0.02423 (7)
Br2	0.40531 (3)	0.04112 (2)	0.85749 (3)	0.02935 (7)
Br3	0.22167 (3)	0.26274 (2)	0.48667 (2)	0.02803 (7)
Br4	0.34474 (3)	0.42516 (2)	0.65020 (3)	0.03093 (7)
Br5	0.21775 (3)	0.60657 (2)	0.48962 (3)	0.03010 (7)
Br6	0.08858 (3)	0.45787 (2)	0.29799 (3)	0.03033 (7)
O1	0.4355 (2)	0.43322 (13)	0.91634 (18)	0.0320 (5)
O2	0.60068 (18)	0.37370 (14)	0.94057 (17)	0.0273 (5)
O3	0.16920 (18)	0.07189 (14)	0.5898 (2)	0.0306 (5)
O4	0.33523 (17)	0.05543 (13)	0.56882 (17)	0.0234 (4)
O5	0.18810 (17)	0.60262 (14)	0.76286 (17)	0.0274 (5)
O6	0.09196 (19)	0.70465 (13)	0.64610 (18)	0.0297 (5)
O7	0.42133 (19)	0.60002 (14)	0.83626 (18)	0.0256 (4)
H7A	0.406 (4)	0.6462 (18)	0.799 (3)	0.052 (13)*
H7B	0.4929 (17)	0.594 (3)	0.869 (3)	0.045 (12)*
O8	0.1619 (2)	0.56996 (15)	0.9707 (2)	0.0317 (5)
H8A	0.116 (3)	0.6106 (17)	0.961 (3)	0.031 (10)*
H8B	0.146 (4)	0.536 (2)	1.010 (3)	0.056 (14)*
O9	0.1742 (3)	0.42709 (17)	0.8218 (3)	0.0565 (9)
H9A	0.177 (3)	0.3743 (12)	0.821 (4)	0.085*
H9B	0.1023 (18)	0.429 (2)	0.783 (4)	0.085*
O10	0.0444 (3)	0.2919 (2)	0.7472 (3)	0.0723 (11)
H10A	0.021 (5)	0.274 (4)	0.680 (2)	0.108*
H10B	0.000 (4)	0.271 (4)	0.774 (4)	0.108*
O11	0.3362 (2)	0.7592 (2)	0.7251 (2)	0.0456 (7)
H11A	0.2668 (19)	0.753 (3)	0.713 (4)	0.057 (14)*
H11B	0.348 (5)	0.791 (3)	0.679 (4)	0.10 (2)*
O12	0.0093 (2)	0.69470 (16)	0.9489 (2)	0.0341 (5)
H12A	−0.045 (3)	0.664 (2)	0.948 (4)	0.045 (12)*
H12B	0.032 (4)	0.726 (3)	1.006 (3)	0.076 (17)*
C1	0.4937 (2)	0.37515 (17)	0.8996 (2)	0.0194 (5)
C2	0.4312 (2)	0.30194 (16)	0.8252 (2)	0.0159 (5)
C3	0.4444 (2)	0.21992 (16)	0.8697 (2)	0.0159 (5)
C4	0.3897 (2)	0.15226 (16)	0.8005 (2)	0.0174 (5)
C5	0.3237 (2)	0.16509 (16)	0.6859 (2)	0.0167 (5)
C6	0.3104 (2)	0.24731 (17)	0.6421 (2)	0.0183 (5)
C7	0.3628 (2)	0.31511 (16)	0.7112 (2)	0.0174 (5)
C8	0.2701 (2)	0.09094 (17)	0.6086 (2)	0.0179 (5)

C9	0.1154 (2)	0.62976 (18)	0.6702 (2)	0.0196 (5)
C10	0.0550 (2)	0.56271 (18)	0.5812 (2)	0.0194 (5)
C11	0.0911 (2)	0.54480 (18)	0.4947 (2)	0.0212 (6)
C12	0.0374 (2)	0.48307 (18)	0.4142 (2)	0.0206 (5)

Atomic displacement parameters (Å²)

	U^{11}	U^{22}	U^{33}	U^{12}	U^{13}	U^{23}
Er1	0.01698 (6)	0.01306 (6)	0.01333 (6)	−0.00005 (4)	0.00272 (4)	0.00077 (4)
Br1	0.02666 (15)	0.02368 (14)	0.01605 (13)	0.00183 (11)	0.00162 (11)	0.00077 (10)
Br2	0.03810 (17)	0.01532 (13)	0.02970 (16)	0.00103 (12)	0.00805 (13)	0.00287 (11)
Br3	0.02991 (16)	0.03137 (16)	0.01536 (13)	−0.00545 (12)	0.00091 (11)	0.00117 (11)
Br4	0.04617 (19)	0.01730 (14)	0.02426 (15)	−0.00146 (13)	0.00843 (13)	0.00352 (11)
Br5	0.02511 (15)	0.03419 (17)	0.03360 (16)	−0.01130 (12)	0.01434 (13)	−0.00158 (13)
Br6	0.02646 (15)	0.04207 (18)	0.02597 (15)	−0.00518 (13)	0.01410 (12)	−0.00478 (13)
O1	0.0503 (15)	0.0217 (11)	0.0255 (11)	0.0102 (10)	0.0164 (10)	−0.0037 (9)
O2	0.0253 (11)	0.0292 (11)	0.0241 (10)	−0.0101 (9)	0.0062 (9)	−0.0075 (9)
O3	0.0215 (11)	0.0304 (12)	0.0410 (13)	−0.0077 (9)	0.0134 (10)	−0.0145 (10)
O4	0.0229 (10)	0.0239 (10)	0.0236 (10)	−0.0031 (8)	0.0093 (8)	−0.0105 (8)
O5	0.0223 (11)	0.0307 (11)	0.0192 (10)	−0.0027 (9)	−0.0025 (8)	0.0075 (8)
O6	0.0333 (12)	0.0235 (11)	0.0253 (11)	0.0019 (9)	0.0039 (9)	0.0034 (9)
O7	0.0238 (11)	0.0264 (11)	0.0267 (11)	0.0011 (9)	0.0101 (9)	0.0051 (9)
O8	0.0308 (12)	0.0286 (12)	0.0410 (13)	0.0127 (10)	0.0198 (11)	0.0143 (10)
O9	0.0589 (19)	0.0343 (15)	0.0499 (17)	−0.0264 (14)	−0.0068 (14)	0.0031 (13)
O10	0.094 (3)	0.075 (2)	0.0420 (17)	−0.057 (2)	0.0201 (17)	−0.0184 (16)
O11	0.0333 (15)	0.0563 (18)	0.0401 (15)	−0.0100 (13)	0.0067 (12)	0.0124 (13)
O12	0.0307 (13)	0.0340 (13)	0.0385 (14)	0.0013 (10)	0.0145 (11)	−0.0060 (11)
C1	0.0285 (15)	0.0143 (12)	0.0145 (12)	−0.0036 (11)	0.0075 (11)	−0.0018 (10)
C2	0.0153 (12)	0.0151 (12)	0.0170 (12)	0.0006 (9)	0.0058 (10)	−0.0041 (10)
C3	0.0151 (12)	0.0173 (12)	0.0141 (12)	0.0040 (10)	0.0044 (10)	−0.0013 (9)
C4	0.0189 (13)	0.0125 (12)	0.0206 (13)	0.0012 (10)	0.0076 (10)	−0.0001 (10)
C5	0.0174 (12)	0.0158 (12)	0.0168 (12)	−0.0017 (10)	0.0067 (10)	−0.0054 (10)
C6	0.0192 (13)	0.0202 (13)	0.0135 (12)	0.0000 (10)	0.0044 (10)	−0.0007 (10)
C7	0.0209 (13)	0.0142 (12)	0.0175 (12)	0.0010 (10)	0.0079 (10)	0.0003 (9)
C8	0.0193 (13)	0.0170 (12)	0.0157 (12)	−0.0014 (10)	0.0051 (10)	−0.0035 (10)
C9	0.0145 (12)	0.0249 (14)	0.0181 (13)	−0.0010 (10)	0.0049 (10)	0.0052 (11)
C10	0.0150 (12)	0.0217 (13)	0.0169 (13)	0.0010 (10)	0.0012 (10)	0.0045 (10)
C11	0.0153 (13)	0.0249 (14)	0.0219 (14)	−0.0029 (11)	0.0055 (11)	0.0042 (11)
C12	0.0192 (13)	0.0258 (14)	0.0158 (12)	−0.0005 (11)	0.0056 (10)	0.0046 (10)

Geometric parameters (Å, º)

Er1—O1	2.266 (2)	O8—H8B	0.820 (19)
Er1—O2^{i}	2.326 (2)	O9—H9A	0.837 (18)
Er1—O4^{ii}	2.333 (2)	O9—H9B	0.852 (18)
Er1—O5	2.238 (2)	O10—H10A	0.845 (14)
Er1—O7	2.347 (2)	O10—H10B	0.842 (14)
Er1—O8	2.297 (2)	O11—H11A	0.838 (19)

Er1—O9	2.323 (3)	O11—H11B	0.84 (2)
Br1—C3	1.891 (3)	O12—H12A	0.848 (19)
Br2—C4	1.888 (3)	O12—H12B	0.835 (19)
Br3—C6	1.891 (3)	C1—C2	1.516 (4)
Br4—C7	1.889 (3)	C2—C3	1.404 (4)
Br5—C11	1.906 (3)	C2—C7	1.399 (4)
Br6—C12	1.898 (3)	C3—C4	1.394 (4)
O1—C1	1.251 (3)	C4—C5	1.398 (4)
O2—C1	1.250 (4)	C5—C6	1.403 (4)
O3—C8	1.245 (3)	C5—C8	1.518 (4)
O4—C8	1.265 (3)	C6—C7	1.387 (4)
O5—C9	1.265 (3)	C9—C10	1.531 (4)
O6—C9	1.233 (3)	C10—C11	1.394 (4)
O7—H7A	0.853 (19)	C10—C12^{iii}	1.401 (4)
O7—H7B	0.843 (19)	C11—C12	1.394 (4)
O8—H8A	0.841 (18)		

O1—Er1—O2^{i}	107.08 (8)	O1—C1—C2	118.3 (3)
O1—Er1—O4^{ii}	73.11 (8)	O2—C1—O1	124.0 (3)
O1—Er1—O7	75.24 (9)	O2—C1—C2	117.7 (2)
O1—Er1—O8	147.57 (8)	C3—C2—C1	120.0 (2)
O1—Er1—O9	83.53 (11)	C7—C2—C1	120.4 (2)
O2^{i}—Er1—O4^{ii}	80.38 (8)	C7—C2—C3	119.6 (2)
O2^{i}—Er1—O7	80.84 (8)	C2—C3—Br1	119.45 (19)
O4^{ii}—Er1—O7	136.20 (8)	C4—C3—Br1	120.6 (2)
O5—Er1—O1	126.07 (8)	C4—C3—C2	120.0 (2)
O5—Er1—O2^{i}	109.61 (8)	C3—C4—Br2	121.2 (2)
O5—Er1—O4^{ii}	150.60 (8)	C3—C4—C5	120.5 (2)
O5—Er1—O7	73.20 (8)	C5—C4—Br2	118.37 (19)
O5—Er1—O8	78.73 (9)	C4—C5—C6	119.2 (2)
O5—Er1—O9	79.14 (9)	C4—C5—C8	120.7 (2)
O8—Er1—O2^{i}	78.15 (9)	C6—C5—C8	120.1 (2)
O8—Er1—O4^{ii}	76.44 (8)	C5—C6—Br3	118.34 (19)
O8—Er1—O7	136.54 (8)	C7—C6—Br3	121.1 (2)
O8—Er1—O9	81.35 (12)	C7—C6—C5	120.5 (2)
O9—Er1—O2^{i}	155.44 (11)	C2—C7—Br4	119.9 (2)
O9—Er1—O4^{ii}	81.79 (9)	C6—C7—Br4	119.9 (2)
O9—Er1—O7	123.64 (11)	C6—C7—C2	120.2 (2)
C1—O1—Er1	169.2 (2)	O3—C8—O4	127.0 (2)
C1—O2—Er1^{i}	117.13 (18)	O3—C8—C5	118.5 (2)
C8—O4—Er1^{iv}	134.39 (18)	O4—C8—C5	114.5 (2)
C9—O5—Er1	169.8 (2)	O5—C9—C10	116.0 (2)
Er1—O7—H7A	127 (3)	O6—C9—O5	125.4 (3)
Er1—O7—H7B	118 (3)	O6—C9—C10	118.6 (2)
H7A—O7—H7B	109 (4)	C11—C10—C9	121.0 (2)
Er1—O8—H8A	137 (2)	C11—C10—C12^{iii}	118.3 (3)
Er1—O8—H8B	116 (3)	C12^{iii}—C10—C9	120.6 (2)
H8A—O8—H8B	107 (4)	C10—C11—Br5	118.2 (2)

Er1—O9—H9A	134 (2)	C12—C11—Br5	120.5 (2)
Er1—O9—H9B	132 (2)	C12—C11—C10	121.3 (3)
H9A—O9—H9B	94 (3)	C10^{iii}—C12—Br6	118.6 (2)
H10A—O10—H10B	106 (4)	C11—C12—Br6	121.1 (2)
H11A—O11—H11B	114 (5)	C11—C12—C10^{iii}	120.3 (3)
H12A—O12—H12B	111 (4)		

Er1—O1—C1—O2	150.8 (10)	C1—C2—C7—Br4	−1.6 (4)
Er1—O1—C1—C2	−29.2 (13)	C1—C2—C7—C6	176.8 (2)
Er1^{i}—O2—C1—O1	13.9 (4)	C2—C3—C4—Br2	−179.92 (19)
Er1^{i}—O2—C1—C2	−166.12 (17)	C2—C3—C4—C5	1.6 (4)
Er1^{iv}—O4—C8—O3	19.4 (5)	C3—C2—C7—Br4	−179.82 (19)
Er1^{iv}—O4—C8—C5	−159.79 (18)	C3—C2—C7—C6	−1.4 (4)
Er1—O5—C9—O6	174.9 (9)	C3—C4—C5—C6	−1.9 (4)
Er1—O5—C9—C10	−6.6 (13)	C3—C4—C5—C8	176.1 (2)
Br1—C3—C4—Br2	−1.4 (3)	C4—C5—C6—Br3	179.5 (2)
Br1—C3—C4—C5	−179.9 (2)	C4—C5—C6—C7	0.6 (4)
Br2—C4—C5—C6	179.6 (2)	C4—C5—C8—O3	95.4 (3)
Br2—C4—C5—C8	−2.5 (3)	C4—C5—C8—O4	−85.4 (3)
Br3—C6—C7—Br4	0.6 (3)	C5—C6—C7—Br4	179.5 (2)
Br3—C6—C7—C2	−177.8 (2)	C5—C6—C7—C2	1.1 (4)
Br5—C11—C12—Br6	0.4 (3)	C6—C5—C8—O3	−86.7 (3)
Br5—C11—C12—C10^{iii}	179.4 (2)	C6—C5—C8—O4	92.6 (3)
O1—C1—C2—C3	−117.9 (3)	C7—C2—C3—Br1	−178.5 (2)
O1—C1—C2—C7	64.0 (4)	C7—C2—C3—C4	0.1 (4)
O2—C1—C2—C3	62.2 (3)	C8—C5—C6—Br3	1.5 (3)
O2—C1—C2—C7	−116.0 (3)	C8—C5—C6—C7	−177.4 (2)
O5—C9—C10—C11	−98.5 (3)	C9—C10—C11—Br5	−0.3 (4)
O5—C9—C10—C12^{iii}	80.6 (3)	C9—C10—C11—C12	179.1 (3)
O6—C9—C10—C11	80.1 (4)	C10—C11—C12—Br6	−179.1 (2)
O6—C9—C10—C12^{iii}	−100.8 (3)	C10—C11—C12—C10^{iii}	0.0 (5)
C1—C2—C3—Br1	3.3 (3)	C12^{iii}—C10—C11—Br5	−179.5 (2)
C1—C2—C3—C4	−178.1 (2)	C12^{iii}—C10—C11—C12	0.0 (5)

Symmetry codes: (i) −*x*+1, −*y*+1, −*z*+2; (ii) *x*, −*y*+1/2, *z*+1/2; (iii) −*x*, −*y*+1, −*z*+1; (iv) *x*, −*y*+1/2, *z*−1/2.

Hydrogen-bond geometry (Å, º)

D—H···*A*	*D*—H	H···*A*	*D*···*A*	*D*—H···*A*
O7—H7*A*···O11	0.86 (3)	2.06 (3)	2.892 (4)	165 (5)
O7—H7*B*···O4^{v}	0.84 (3)	2.10 (3)	2.931 (4)	168 (4)
O8—H8*A*···O12	0.84 (3)	1.86 (3)	2.705 (4)	174 (3)
O8—H8*B*···O3^{ii}	0.82 (4)	1.96 (3)	2.703 (3)	152 (5)
O9—H9*A*···O10	0.84 (2)	2.05 (4)	2.643 (5)	128 (4)
O10—H10*A*···O12^{vi}	0.85 (3)	2.00 (5)	2.808 (4)	160 (5)
O10—H10*B*···O6^{vi}	0.84 (5)	2.12 (6)	2.948 (5)	171 (6)
O11—H11*A*···O6	0.84 (3)	2.18 (4)	2.989 (4)	161 (5)
O11—H11*B*···O2^{v}	0.84 (5)	2.31 (5)	3.139 (4)	174 (6)

O12—H12*A*···O3^{vii}	0.84 (4)	2.06 (4)	2.879 (4)	164 (4)
O12—H12*B*···O6^{viii}	0.84 (4)	1.99 (4)	2.832 (3)	177 (4)

Symmetry codes: (ii) x, $-y+1/2$, $z+1/2$; (v) $-x+1$, $y+1/2$, $-z+3/2$; (vi) $-x$, $y-1/2$, $-z+3/2$; (vii) $-x$, $y+1/2$, $-z+3/2$; (viii) x, $-y+3/2$, $z+1/2$.